

# Orienting molecules using half-cycle pulses

C.M. Dion<sup>1,2,a</sup>, A. Keller<sup>1</sup>, and O. Atabek<sup>1,b</sup><sup>1</sup> Laboratoire de Photophysique Moléculaire du CNRS, bâtiment 213, campus d'Orsay, 91405 Orsay, France<sup>2</sup> Laboratoire Aimé Cotton, CNRS, bâtiment 505, campus d'Orsay, 91405 Orsay, France

Received 16 August 2000 and Received in final form 4 December 2000

**Abstract.** Using a rigid-rotor model, we study the orientation dynamics of polar diatomic molecules excited by experimentally available half-cycle pulses. The results of the numerical solution of the time-dependent Schrödinger equation are compared to those of an approximate “sudden-impact” impulsive model neglecting the molecular rotation during the pulse. We show that efficient orientation is achieved during time periods of several picoseconds for LiCl. For short pulses, where the kicked molecule model is valid, orientation turns out to be mainly sensitive to the time-integrated field amplitude and not the shape or rise time of the pulse.

**PACS.** 33.80.-b Photon interactions with molecules – 32.80.Lg Mechanical effects of light on atoms, molecules, and ions

## 1 Introduction

Molecular orientation is one of the most important goals in the study of chemical reaction dynamics due to the high sensitivity of reaction cross-sections, in bi-molecular collisions, to the relative orientation of the two collision partners [1–3]. Alignment and especially orientation are needed in controlling laser-induced isomerization [4], for isotope separation [5], for photofragment analysis [6], for molecular trapping [7, 8], surface processing [7] or catalysis [9], and for nanoscale design by laser focusing of molecular beams [7, 10]. Consequently, recent experimental and theoretical efforts to achieve control of molecular orientation raised considerable interest. The hexapole state selection [11, 12] and the so-called “brute force” orientation techniques [3, 13] have, in particular, been used for orienting, in a DC electric field, molecules with a permanent dipole moment. Optimal and coherent control schemes have also been proposed. A properly tailored microwave pulse, with reasonable peak power, offers, in principle, the possibility to orient, in a temporally recurrent way, a polar diatomic molecule initially in the isotropic  $J = M_J = 0$  state [14]. Computer simulations show, in a coherent control scenario, that picosecond two-color phase-locked laser excitation of heteronuclear diatomic molecules can also provide orientation during or after the laser pulse [15]. Another possible orientation scheme of polar molecules is based on the simultaneous action of both permanent-dipole- and polarizability-field interactions enhanced by intense linearly-polarized infrared pulses combining a fun-

damental frequency  $\omega$  and its second harmonic  $2\omega$ , where  $2\omega$  is resonant with a vibrational transition. Numerical simulations carried on a triatomic system, namely HCN, lead to orientation when the laser is turned off, basically due to symmetry breaking effects [16].

Recently it has become possible to generate extremely short electrical pulses with peak fields of up to 150 kV/cm [17]. They present a large asymmetry in the magnitude of positive and negative electric field components, such that, to a reasonable approximation, they can be considered as half-cycle pulses (HCP) rather than single-cycle. The picture is that of a short (sub-picosecond) unipolar pulse followed by a very long and weak tail of opposite electric field. This tail may last tens of picoseconds but with an amplitude at least ten times less than the one of the main peak. The frequency spectrum extends up to 2 THz, corresponding to a short duration (0.5 to 1 ps) as compared to the timescales of molecular rotational motion. In a short-pulse (impulsive) limit, the radiative interaction can best be described as a kick. The ionization of Rydberg atoms under the effect of HCPs [18, 19], of brief duration with respect to the Kepler orbit of the Rydberg electron, is interpreted in terms of a kinetic momentum rapidly transferred to the electron and given by the (non-zero) time-integrated electric field [20–22]. In molecular dynamics, alignment enhancement is obtained in the sudden approximation regime. An HCP, which is short compared to rotational periods, could impart a kick on the molecule and transfer angular momentum. The consequence would be angular motion in the direction of the kick [23, 24]. Alignment and even orientation of photofragments can also be obtained using intense half-cycle and few-cycle laser pulses [25].

---

<sup>a</sup> e-mail: [claude.dion@lac.u-psud.fr](mailto:claude.dion@lac.u-psud.fr)<sup>b</sup> e-mail: [osman.atabek@ppm.u-psud.fr](mailto:osman.atabek@ppm.u-psud.fr)

In this article, we precisely make use of the two characteristics of HCPs, namely their impulsive, sudden nature and their highly asymmetric shape to transfer angular momentum to the molecule and to investigate their ability at producing molecular orientation. Section 2 introduces a time-dependent Schrödinger equation (TDSE) theory within the frame of a rigid-rotor description of the molecule and the radiative HCP interaction written in the dipole approximation. This is complemented by a sudden-impact approximation (impulsive model) which, in particular, shows that the HCP-induced dynamics are only sensitive to the time-integrated electric field (and not the shape or rise time of the HCP). The results of numerical simulations on the model molecule LiCl are presented in Section 3, where the possibility of recurrent orientation over time periods of several picoseconds, during and after the pulse, is evidenced and we discuss the role of the HCP's tail. A summary and some prospects are presented in the conclusion.

## 2 Theory

### 2.1 Model

We consider a diatomic molecule within a rigid-rotor approximation (frozen internal vibrational motion) interacting with an electromagnetic field. The complete molecule-plus-field Hamiltonian for this model is

$$\hat{H} = B\hat{J}^2 + V_{\mathcal{E}}(\theta, t), \quad (1)$$

where  $\hat{J}^2$  is the angular momentum operator and  $B$  the rotational constant ( $B = \hbar^2/2I$ ,  $I$  being the moment of inertia calculated for the fixed internuclear distance). The time-dependent part,  $V_{\mathcal{E}}(\theta, t)$ , represents the radiative interaction given by

$$V_{\mathcal{E}}(\theta, t) = -\boldsymbol{\mu} \cdot \boldsymbol{\mathcal{E}}(t), \quad (2)$$

$\theta$  being the angle between the molecular dipole moment  $\boldsymbol{\mu}$  and the electric field vector  $\boldsymbol{\mathcal{E}}(t)$  of the linearly polarized HCP. It is precisely this angle which defines the orientation of the molecule with respect to the electric field and, consequently, to the laboratory reference frame. In the presence of an electric field, the dipole moment can be expanded in terms of a series of powers of  $\boldsymbol{\mathcal{E}}$ . For non-oscillating and relatively moderate field strengths, as is the case of HCPs, only the first term of this series (*i.e.*,  $\mu_0$ , the permanent dipole moment) is retained (the dipole induced by the field through the polarizability is neglected) [26]. Finally, the TDSE for this model is given by

$$i\hbar \frac{\partial}{\partial t} \Psi(\theta, \varphi; t) = \left[ B\hat{J}^2 - \mu_0 \mathcal{E}(t) \cos \theta \right] \Psi(\theta, \varphi; t), \quad (3)$$

$\varphi$  being the azimuthal angle. The initial state (at  $t = 0$ ) is taken as the isotropic, ground rotational state  $J = M_J = 0$ , where  $M_J$ , the projection of the total angular momentum  $J$  on the field polarization axis, is a good quantum

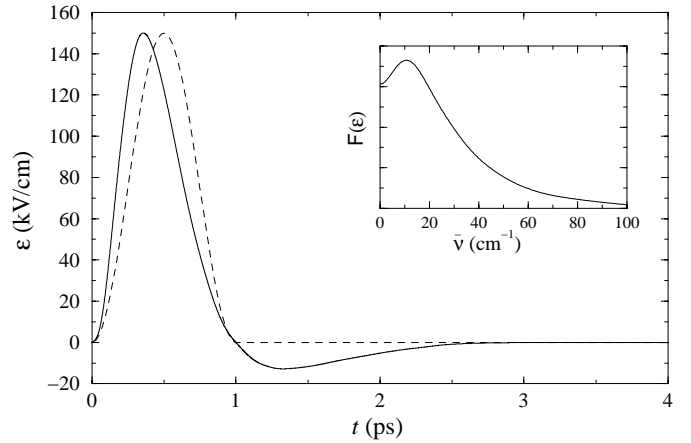


**Fig. 1.** Electric field of the far-infrared half-cycle pulse as a function of time, taken from reference [17] (solid line) and sine-square unidirectional pulse with equivalent maximum amplitude and duration (dashed line). Inset: Fourier transform of the half-cycle pulse.

number which remains constant during the excitation (selection rule  $\Delta M_J = 0$ ). Numerical solutions for the wave function propagation of equation (3) are obtained by the application, within each time slice  $[t, t + \delta t]$ , of a third-order split-operator method [27,28] in conjunction with the scheme developed by Dateo and Metiu [29,30] for angular variables.

The orientation dynamics are observed through the time-dependent angular distribution given by

$$\mathcal{P}(\theta; t) = \int_0^{2\pi} |\Psi(\theta, \varphi; t)|^2 d\varphi. \quad (4)$$

An average quantitative measure of orientation can be taken as the expectation value of  $\cos \theta$  [13,31]:

$$\langle \cos \theta \rangle = \int_0^\pi \mathcal{P}(\theta; t) \cos \theta \sin \theta d\theta. \quad (5)$$

Orientation is obtained for large absolute values of  $\langle \cos \theta \rangle$ . It is worthwhile noting that alignment cannot be measured by  $\langle \cos \theta \rangle$  (the expectation value of  $\cos^2 \theta$  remains a possible measure). In the following, it is the time-dependent behavior of  $\langle \cos \theta \rangle$  which is taken for measuring molecular orientation.

### 2.2 Description of the half-cycle pulses

The electric fields used in our calculations are picosecond far-infrared electromagnetic pulses experimentally generated when illuminating a GaAs wafer, in the presence of a pulsed electric field applied across the surface, by a Ti:sapphire laser [17]. Figure 1 displays the time-dependent electric field  $\mathcal{E}(t)$  of an HCP, taken from Figure 3 of reference [17], together with an analytical form,

$$\mathcal{E}(t) = \begin{cases} \mathcal{E}_0 \sin^2(\pi t/t_p) & \text{if } 0 \leq t \leq t_p \\ 0 & \text{elsewhere} \end{cases}, \quad (6)$$

which fits the main features of the experimental shape (peak amplitude  $\mathcal{E}_0$ , duration  $t_p$ , full width at half maximum FWHM) except the tail which is dropped. (When considering an HCP with a tail,  $t_p$  will again be taken as the duration of the positive amplitude part of the pulse, *i.e.*, will correspond to the time at which the electric field changes sign.) Concerning the experimental HCP, the following points have to be noticed:

- (i) the maximum field amplitude that can so far be achieved,  $\mathcal{E}_0 \sim 150$  kV/cm, corresponds to a peak intensity of the order of  $10^8$  W/cm<sup>2</sup>. This is low enough that no ionization is expected for typical diatomic molecules in their ground electronic state. For instance, the ionization potential of LiCl is 9.57 eV [32], so the field threshold for ionization predicted from tunneling ionization models [33],  $\mathcal{E}_i = 1.6 \times 10^8$  V/cm, remains high enough, such that HCPs with these characteristics can be used without risk of damage to the molecule;
- (ii) although the central frequency  $\omega \approx 0.3$  THz ( $\bar{\nu} \approx 11$  cm<sup>-1</sup>, see inset of Fig. 1) is out of resonance with respect to molecular rotation frequencies  $\omega_{\text{rot}} = 2B/\hbar$  (of the order of  $10^{10}$  Hz, corresponding to a few cm<sup>-1</sup>), the FWHM ( $\sim 1$  THz or  $\sim 30$  cm<sup>-1</sup>) is broad enough to provide non-negligible field components at  $\omega_{\text{rot}}$  that induce rotational transitions;
- (iii) when neglecting the very smooth tail, the field duration,  $t_p = 1$  ps, is short enough with respect to typical molecular rotational periods  $T_{\text{rot}} = \hbar/2B$  (of the order of tens of picoseconds) that a sudden approximation within an impulsive model can be considered as valid;
- (iv) the short unipolar pulse is followed by a very long, weak tail of opposite electric field with a marked asymmetry between the maximum and the minimum at either side. This tail typically lasts tens of picoseconds and has an amplitude of 10% or less than the main peak (an amplitude asymmetry of approximately 12:1 is observed in Fig. 1). Strictly, the electric field for a freely propagating electromagnetic pulse must integrate to zero, be it over a very long time (in the case of the HCP shown in Fig. 1, the area of the tail, integrated up to  $t = 4$  ps, represents 15% of the area of the main peak). However, a transfer of angular momentum should take place on the timescale of the short pulse where the electric field is essentially unidirectional [23, 24], and the effect of the long weak tail should be negligible.

### 2.3 Impulsive limit: sudden-impact approximation

The impulsive limit basically reflects the fact that during the short HCP (without taking into account the tail) the molecular rotational motion can approximatively be neglected. We look for a solution of equation (3) for a wave function  $\tilde{\Psi}(\theta, \varphi; t)$  derived from  $\Psi(\theta, \varphi; t)$  by a unitary transformation involving the rotational kinetic oper-

ator  $B\hat{J}^2$  and defined as

$$\tilde{\Psi}(\theta, \varphi; t) = \exp\left(\frac{i}{\hbar}B\hat{J}^2t\right)\Psi(\theta, \varphi; t). \quad (7)$$

The TDSE for  $\tilde{\Psi}$  is simply written as

$$i\hbar\frac{\partial}{\partial t}\tilde{\Psi}(\theta, \varphi; t) = -\left[\exp\left(\frac{i}{\hbar}B\hat{J}^2t\right)\mu_0\mathcal{E}(t)\cos\theta \times \exp\left(-\frac{i}{\hbar}B\hat{J}^2t\right)\right]\tilde{\Psi}(\theta, \varphi; t) \quad (8)$$

and the transformed wave function  $\tilde{\Psi}(\theta, \varphi; t_p)$  at time  $t_p$  (end of the HCP) is obtained as the solution of the implicit equation

$$\tilde{\Psi}(\theta, \varphi; t_p) = \frac{i\mu_0}{\hbar}\int_0^{t_p}\left[\exp\left(\frac{i}{\hbar}B\hat{J}^2t\right)\mathcal{E}(t)\cos\theta \times \exp\left(-\frac{i}{\hbar}B\hat{J}^2t\right)\right]\tilde{\Psi}(\theta, \varphi; t)dt + \tilde{\Psi}(\theta, \varphi; 0). \quad (9)$$

This derivation is close to the Magnus expansion of the time evolution operator as shown by Henriksen [24]. A lowest order model based on a short pulse approximation, with respect to the rotational period, precisely means that

$$t_p \ll \frac{\hbar}{B\hat{J}^2}. \quad (10)$$

The fulfillment of inequality (10) implies the unity value for the exponential of the unitary transformation, leading to the approximate solution of equation (9):

$$\tilde{\Psi}(\theta, \varphi; t_p) = e^{i\mathcal{A}\cos\theta}\tilde{\Psi}(\theta, \varphi; 0), \quad (11)$$

where  $\mathcal{A}$  is obtained from the integrated electric field in the large half-cycle component of the pulse,

$$\mathcal{A} = \frac{\mu_0}{\hbar}\int_0^{t_p}\mathcal{E}(t)dt. \quad (12)$$

Finally, the wave function solution of equation (3), within this impulsive model, is obtained by combining equations (7, 11) as

$$\Psi(\theta, \varphi; t > t_p) = \exp\left(-\frac{i}{\hbar}B\hat{J}^2t\right)e^{i\mathcal{A}\cos\theta}\Psi(\theta, \varphi; 0). \quad (13)$$

Application of the  $\exp(-iB\hat{J}^2t/\hbar)$  operator at the lowest order shows that the initial isotropy of  $\Psi(\theta, \varphi; 0)$  is no longer conserved: an asymmetry with respect to a change of  $\theta$  into  $\pi - \theta$  is the signature of a possible orientation effect that is analyzed in the following. But the most interesting observation is that, as far as the sudden-impact approximation (Eq. (13)) applies, the orientation depends only on the integrated electric field  $\mathcal{A}$  and is insensitive to the shape and rise time of the HCP (contrary to what may happen if the pulse duration is within the same timescale as molecular motion [34]). The interest of an HCP for orienting a molecule is now clearly evidenced, at least within

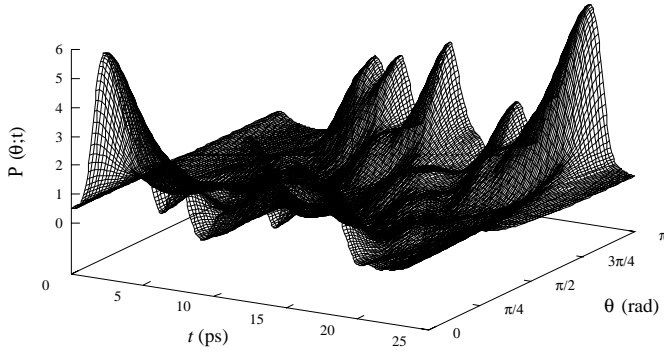


**Fig. 2.** 3D plot of the angular distribution  $\mathcal{P}(\theta; t)$  for  ${}^7\text{Li}^{35}\text{Cl}$  (initial state  $J = M_J = 0$ ) submitted to an HCP of  $\mathcal{E}_0 = 150$  kV/cm peak field and  $t_p = 1$  ps duration.

the frame of the impulsive limit. Actually, in situations where a molecule interacts with a short (as compared to its rotational period) laser pulse, even an asymmetric (*e.g.*,  $\omega + 2\omega$ ) field has a null time-integrated amplitude  $\mathcal{A}$ , so orientation would thus hardly be achieved (see Fig. 3 of Ref. [16]), in the absence of any vibrational or electronic excitation.

### 3 Results

The polar diatomic molecule that is taken as an illustrative example, namely  ${}^7\text{Li}^{35}\text{Cl}$ , is characterized by two parameters, a rather important permanent dipole moment  $\mu_0 = 7.129$  D = 2.805 a.u. (which for most heteronuclear diatomic molecules lies in the range 0.1–10 D) [32] and a rotational constant  $B = 0.70652$  cm $^{-1}$  =  $3.2192 \times 10^{-6}$  a.u. [35] (at the Li–Cl equilibrium distance of 2.02 Å). This allows a large molecule-field coupling during the pulse providing good orientation possibility and slow molecular rotational dynamics after the pulse is turned off (due to the large moment of inertia), so that any orientation is kept for a period of time sufficiently long to eventually perform subsequent measurements. The rotational period  $T_{\text{rot}} = h/2B \approx 23.6$  ps is an order of magnitude longer than the duration of the HCP,  $t_p = 1$  ps, allowing thus the sudden-impact approximation. More precisely, averaging  $\hat{J}^2$  by its eigenvalue  $J(J+1)$ , one gets

$$\frac{B\hat{J}^2 t_p}{\hbar} \approx 0.133J(J+1), \quad (14)$$

which fulfills the requirements of equation (10) in the case where only the lowest  $J$ s are populated, corresponding to rotational temperatures up to  $\sim 5$  K.

The orientation dynamics, resulting from a full numerical solution of equation (3), is given in Figure 2 as a three-dimensional plot of  $\mathcal{P}(\theta; t)$  for an HCP of  $\mathcal{E}_0 = 150$  kV/cm,  $t_p = 1$  ps. At  $t = 0$  ps, we have an isotropic distribution. Excellent orientation is obtained at about 3 ps, with an angular distribution well peaked at  $\theta = 0$  rad and negligible population at  $\theta = \pi$  rad. A completely opposite situation is valid at longer times ( $t \sim 21$  ps) where the angular

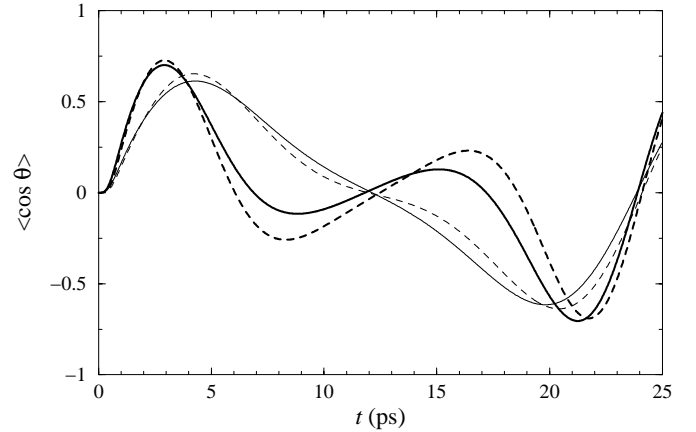


**Fig. 3.** Average value of  $\cos\theta$  as a function of time for  ${}^7\text{Li}^{35}\text{Cl}$  submitted to two HCPs with peak amplitudes  $\mathcal{E}_0 = 150$  kV/cm (solid thin line) and  $\mathcal{E}_0 = 250$  kV/cm (solid thick line) and equivalent- $\mathcal{A}$  sine-squared pulses (see text) with  $\mathcal{E}_0 \approx 144$  kV/cm (dashed thin line) and  $\mathcal{E}_0 \approx 240$  kV/cm (dashed thick line).

distribution is almost completely confined at  $\theta = \pi$  rad, which also means rather good orientation. At intermediate times, there is no orientation (some alignment features can still be observed at  $t = 12$  ps with angular distributions shared between regions close to  $\theta = 0$  or  $\pi$  rad).

The mean values of  $\cos\theta$  as a function of time are displayed in Figure 3 for two HCPs of different peak amplitudes  $\mathcal{E}_0 = 150$  and 250 kV/cm. We also give the behavior of  $\langle \cos\theta \rangle$  for pulses with a sine-squared form (see Eq. (6)) and equal time-integrated electric fields  $\mathcal{A}$  as the positive (principal) components of the corresponding HCPs. Several observations are in order:

- (i) good agreement is obtained when comparing dynamics induced by HCPs and equivalent- $\mathcal{A}$  sine-squared pulses. This is a first indication that the tail of HCPs does not play an important part;
- (ii) orientation is only partially achieved while the pulse is on (with  $\langle \cos\theta \rangle$  reaching values of the order of 0.2 at  $t = 1$  ps) but continues to grow after the pulse has passed ( $\langle \cos\theta \rangle$  reaching  $\sim 0.7$  at  $t = 2.9$  ps for the strongest field). Efficient orientation (with  $\langle \cos\theta \rangle$  larger than 0.5) lasts for several picoseconds and occurs recurrently with a period of about 24 ps, corresponding to the molecular rotational period, with some strong but spatially inverted orientation also present;
- (iii) stronger fields lead to better orientation but for shorter durations. More precisely, maximum orientation changes from  $\langle \cos\theta \rangle = 0.70$  to  $\langle \cos\theta \rangle = 0.61$  when  $\mathcal{E}_0$  varies from 250 kV/cm to 150 kV/cm, while the orientation time (during which  $\langle \cos\theta \rangle$  is larger than 0.5) changes from 2.8 ps to 3.6 ps.

A quantitative analysis of the role played by the tail deserves special attention, as one expects that in orientation dynamics this very long duration and smooth negative component of the HCP has negligible effects,

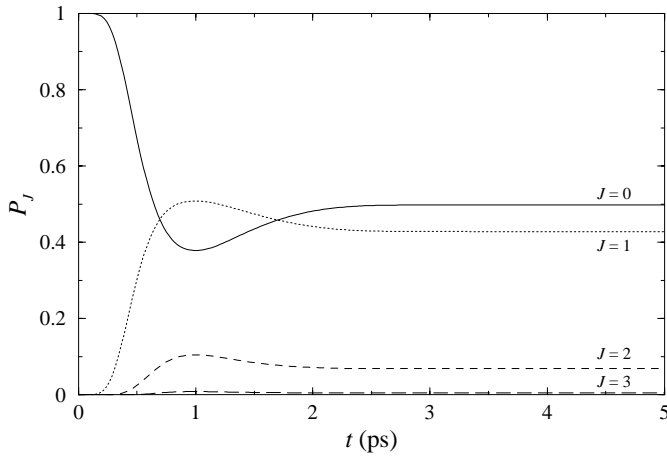


**Fig. 4.** LiCl rotational population distribution as a function of time using an HCP with peak amplitude  $\mathcal{E}_0 = 150$  kV/cm and pulse duration  $t_p = 1$  ps.

due to its weak field amplitude and adiabatic behavior with respect to rotational excitation. In other words, although the time-integrated amplitude of this negative component has to cancel the short duration positive component, its adiabatic action is such that the rotational population distribution can basically no longer be modified after a time  $\tau$  when its amplitude is small enough. Figure 4 shows the time evolution of the rotational populations,

$$P_J(t) = |\langle J, 0 | \Psi(t) \rangle|^2, \quad (15)$$

obtained by projecting the wave function of equation (3) on the spherical harmonics  $|J, 0\rangle \equiv Y_{J,0}(\theta, \varphi)$ , for an HCP with  $\mathcal{E}_0 = 150$  kV/cm and  $t_p = 1$  ps. For such a pulse, we observe that only a few rotational states are populated (up to  $J = 3$ ). At time  $t = t_p = 1$  ps, the normalized rotational distribution is roughly stabilized with  $P_0 \approx 0.38$ ,  $P_1 \approx 0.51$ , and  $P_2 \approx 0.11$ . The subsequent action of the tail gives rise to changes of the order of 0.1 in the populations, and the final distribution is obtained within excellent accuracy at a time  $\tau$  which does not exceed 3 ps, with  $P_0 \approx 0.50$ ,  $P_1 \approx 0.43$ , and  $P_2 \approx 0.07$ , all other populations being less than 0.01. An even more quantitative determination of  $\tau$  can be deduced from the stabilization of the average value of  $\cos\theta$  as a function of time by truncating the tail at different times. This can be done by simulating a truncated HCP by a sine-squared pulse (6) presenting the same  $\mathcal{A}$  as the truncated HCP under consideration (with  $t_p = 1$  ps), *i.e.*, taking a value of  $\mathcal{E}_0$  for the sine-squared pulse such that its time-integrated electric field amplitude  $\mathcal{A}_{\text{sin}^2} = \mu_0 \mathcal{E}_0 t_p / 2\hbar$  is the same as the value  $\mathcal{A}_{\text{HCP}}$  obtained by numerically integrating the HCP over the range  $[0, \tau]$ . The root-mean-square of the difference between  $\langle \cos\theta \rangle^{\text{HCP}}$  (calculated for the full HCP) and  $\langle \cos\theta \rangle^\tau$  (calculated for the sine-squared pulse

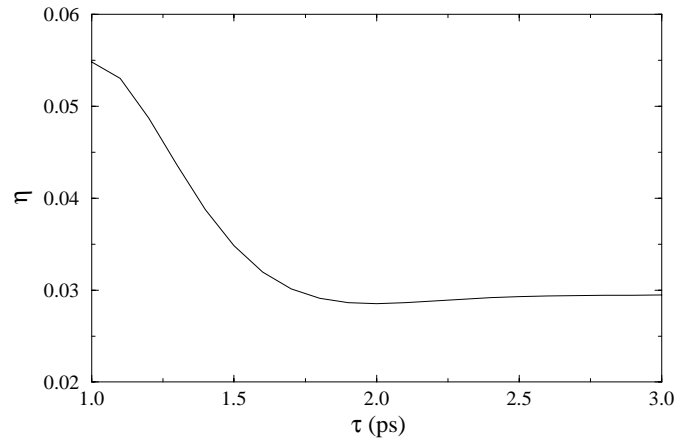


**Fig. 5.** Root-mean-square of the differences in the values of  $\langle \cos\theta \rangle$  resulting from truncated HCPs as a function of the truncation time  $\tau$  (see text).

just described), defined as

$$\eta(\tau) = \left( \frac{1}{T_{\text{rot}}} \int_0^{T_{\text{rot}}} |\langle \cos\theta \rangle^{\text{HCP}}(t) - \langle \cos\theta \rangle^\tau(t)|^2 dt \right)^{1/2}, \quad (16)$$

is given in Figure 5 as a function of the truncation time  $\tau$ . One observes a fast decrease of  $\eta$ , with an almost negligible value (less than  $3 \times 10^{-2}$ ) for  $\tau = 2$  ps, supporting thus the expectation of a negligible contribution of the long-time behavior of HCPs on molecular rotation dynamics. Nevertheless, as the results for  $\eta(\tau)$  show, and as was also evidenced by the comparison between the HCPs and sine-squared pulses in Figure 3, the tail does have an influence on the effective value of  $\mathcal{A}$ : it reduces the overall kick felt by the molecule.

Finally, the ability of the lowest order sudden-impact model to produce approximate angular distributions in the case of LiCl excited with experimentally achievable HCPs is examined in Figure 6, where we compare the result obtained by the exact solution of equation (3) with  $\mathcal{E}_0 = 150$  kV/cm and  $t_p = 1$  ps to the result obtained from equation (13) with  $\mathcal{A} \approx 1.42$ , corresponding to  $\tau = 2$  ps. Although equation (14) provides a rather high estimation of  $B\hat{j}_p^2 t_p / \hbar$  within the validity domain of the approximation, it turns out that the final ( $t = 25$  ps) rotational distributions  $P_J$  resulting from the exact and approximate calculations are almost identical (the absolute differences do not exceed 0.015). As for the dynamical behavior of  $\langle \cos\theta \rangle$  obtained from both calculations, the agreement is still very satisfactory. The slight difference is basically due to the finite time  $t_p$  of the kick (not quite small enough with respect to the rotational period), which induced a phase shift in the values of the rotational coefficients. The overall orientation characteristics are well reproduced with a quantitative agreement of  $\eta = 0.033$  in terms of the root-mean-square defined in equation (16). This contributes to show that, for a large class of molecules, excited with

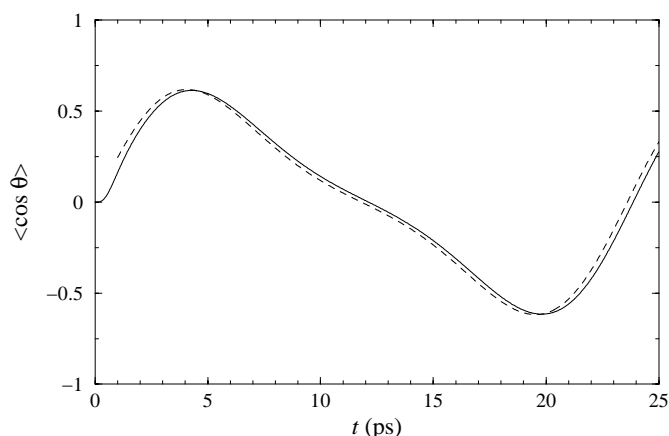


**Fig. 6.** Average value of  $\cos \theta$  for  ${}^7\text{Li}^{35}\text{Cl}$  submitted to an HCP with  $\mathcal{E}_0 = 150$  kV/cm and  $t_p = 1$  ps. Solid line: exact calculation; dashed line: lowest-order impulsive model approximation (for  $\tau = 2$  ps,  $\mathcal{A} \approx 1.42$ ).

experimentally achievable HCPs, orientation may be obtained within the frame of a kicked molecule model where the dynamics depend mainly on the time-integrated electric field and not on the pulse shape or rise time, as far as the HCP remains adiabatic with respect to other degrees of freedom.

## 4 Conclusion

We have shown in this paper that an HCP can induce orientation in a polar molecule by creating a coherent superposition of its rotational eigenstates. Such pulses, experimentally available, present a unipolar large amplitude, short duration component followed by an opposite-polarity negative weak-amplitude and very long duration tail, strictly resulting into a null time-integrated amplitude. The large-amplitude unipolar component imparts a kick to the molecule which, because of the unidirectionality and the strength of the field, may be efficiently oriented with  $\langle \cos \theta \rangle > 0.7$ . The adiabatic behavior, with respect to rotational motion, of the weak amplitude component (the HCP's tail) is such that its effect on the dynamics is limited to changes less than 0.1 in the rotational populations. The orientation lasts a time which depends on the molecular rotation period and, for a molecule like LiCl with a large moment of inertia, this may amount to several picoseconds. The orientation occurs recurrently with the periodicity of molecular rotations, *i.e.*, the molecule remains periodically oriented even in the absence of any external field. This represents an advantage over other orientation techniques, such as the brute force method [3,13], where the molecule is only oriented when the field is present.

The application of an impulsive “sudden-impact” model at lowest order, while freezing rotational dynamics during the pulse (*i.e.*, the large amplitude component of the HCP), leads to rotational populations and angular distributions within fairly good accuracy. This, in particular, shows that the dynamics are, at least for short

pulses, mainly sensitive to the time-integrated field amplitude (partly neglecting the HCP's tail) and not to its shape or rise time.

Our calculations have so far been carried out using a rigid-rotor model for the molecule, starting from the ground rotational state  $J = M_J = 0$ . The feasibility of orienting molecules using HCPs has to be checked against the initial rotational temperature and the coupling of the internal vibrational and rotational motions. The exploration of the effect of HCPs on vibrating molecules as well as on heavier systems such as RbCl is currently under investigation in our group. Orienting molecules and *a fortiori* controlling their orientation remains an important goal on which we are actively working by examining the role of experimentally achievable HCP trains [36] or by referring to optimal control schemes to tailor a laser pulse using automatic differentiation algorithms [37].

We are grateful to Pr. Benoît Soep for stimulating discussions. We acknowledge the financial support of the Natural Sciences and Engineering Council of Canada (to C.M.D.) and of the *Action Concertée Incitative Blanche* “Study of the laser control of chemical reactions” from the French Ministry of Research.

## References

1. P.R. Brooks, *Science* **193**, 11 (1976).
2. A.H. Zewail, *J. Chem. Soc. Faraday Trans. 2* **85**, 1221 (1989).
3. H.J. Loesch, A. Remscheid, *J. Chem. Phys.* **93**, 4779 (1990).
4. C.M. Dion, S. Chelkowski, A.D. Bandrauk, H. Umeda, Y. Fujimura, *J. Chem. Phys.* **105**, 9083 (1996).
5. E. Charron, A. Giusti-Suzor, F.H. Mies, *Phys. Rev. A* **49**, R641 (1994).
6. A.D. Bandrauk, E.E. Aubanel, *Chem. Phys.* **198**, 159 (1995).
7. T. Seideman, *Phys. Rev. A* **56**, R17 (1997).
8. H. Abou-Rachid, T.T. Nguyen-Dang, O. Atabek, *J. Chem. Phys.* **110**, 4737 (1999); *ibid.* **114**, 2197 (2001).
9. M.G. Tenner, E.W. Kuipers, A.W. Kleyn, S. Stolte, *J. Chem. Phys.* **94**, 5197 (1991), and references therein.
10. H. Stapelfeldt, H. Sakai, E. Constant, P.B. Corkum, *Phys. Rev. Lett.* **79**, 2787 (1997).
11. K.H. Kramer, R.B. Bernstein, *J. Chem. Phys.* **42**, 767 (1965).
12. T.D. Hain, R.M. Moision, T.J. Curtiss, *J. Chem. Phys.* **111**, 6797 (1999), and references therein.
13. B. Friedrich, D.R. Herschbach, *Z. Phys. D* **18**, 153 (1991).
14. R.S. Judson, K.K. Lehmann, H. Rabitz, W.S. Warren, *J. Mol. Spectrosc.* **223**, 425 (1990).
15. M.J.J. Vrakking, S. Stolte, *Chem. Phys. Lett.* **271**, 209 (1997).
16. C.M. Dion, A.D. Bandrauk, O. Atabek, A. Keller, H. Umeda, Y. Fujimura, *Chem. Phys. Lett.* **302**, 215 (1999).
17. D. You, R.R. Jones, P.H. Bucksbaum, D.R. Dykaar, *Opt. Lett.* **18**, 290 (1993).

18. R.R. Jones, D. You, P.H. Bucksbaum, *Phys. Rev. Lett.* **70**, 1236 (1993).
19. P.H. Bucksbaum, in *The Physics and Chemistry of Wave Packets*, edited by J.A. Yeazell, T. Uzer (Wiley, New York, 2000).
20. C.O. Reinhold, M. Melles, H. Shao, J. Burgdörfer, *J. Phys. B: At. Mol. Opt. Phys.* **26**, L659 (1993).
21. R.B. Vrijen, G.M. Lankhuijzen, L.D. Noordam, *Phys. Rev. Lett.* **79**, 617 (1997).
22. O. Zobay, G. Alber, *Phys. Rev. A* **60**, 1314 (1999).
23. T. Seideman, *Phys. Rev. Lett.* **83**, 4971 (1999).
24. N.E. Henriksen, *Chem. Phys. Lett.* **312**, 196 (1999).
25. J.T. Lin, S.H. Lin, T.F. Jiang, *Phys. Rev. A* **61**, 033407 (2000).
26. C.M. Dion, A. Keller, O. Atabek, A.D. Bandrauk, *Phys. Rev. A* **59**, 1382 (1999).
27. M.D. Feit, J.A. Fleck Jr, A. Steiger, *J. Comput. Phys.* **47**, 412 (1982).
28. A.D. Bandrauk, H. Shen, *J. Chem. Phys.* **99**, 1185 (1993).
29. C.E. Dateo, H. Metiu, *J. Chem. Phys.* **95**, 7392 (1991).
30. R. Numico, A. Keller, O. Atabek, *Phys. Rev. A* **52**, 1298 (1995).
31. B. Friedrich, D.R. Herschbach, *Nature* **353**, 412 (1991).
32. *CRC Handbook of Chemistry and Physics*, edited by D.R. Lide, 74th edn. (CRC Press, Boca Raton, Fl., 1993).
33. P. Dietrich, P.B. Corkum, D.T. Strickland, M. Laberge, in *Molecules in Laser Fields*, edited by A.D. Bandrauk (Dekker, New York, 1994).
34. B.E. Tannian, R.A. Popple, F.B. Dunning, S. Yoshida, C.O. Reinhold, J. Burgdörfer, *J. Phys. B: At. Mol. Opt. Phys.* **31**, L455 (1998).
35. E.F. Pearson, W. Gordy, *Phys. Rev.* **177**, 52 (1969).
36. M.T. Frey, F.B. Dunning, C.O. Reinhold, S. Yoshida, J. Burgdörfer, *Phys. Rev. A* **59**, 1434 (1999).
37. A. Ben Haj-Yedder, C.M. Dion, A. Keller, O. Atabek, E. Cances, C. Le Bris (in preparation).